# An EXAFS Study on Metal-Substitution Reaction of Homodinuclear Mercury(II) Porphyrin with Copper(II) in Aqueous Solution

Masaaki TABATA* and Kazuhiko OZUTSUMI†
Department of Chemistry, Faculty of Science and Engineering, Saga University, Honjo-machi, Saga 840
† Department of Chemistry, University of Tsukuba, Tsukuba 305

(Received January 14, 1994)

The metal-substitution reaction of the homodinuclear mercury(II) porphyrin complex, $[Hg_2(tpps)]^{2-}$ ($H_2tpps^{4-}$=tetrakis(4-sulfonatophenyl)porphyrin), with copper(II) has been studied by the EXAFS (extended X-ray absorption fine structure) method in an acetate buffer (pH 5.6). The tetrahedral mercury(II) acetato complex ($r_{Hg-O}=219$ pm, $r_{Hg-O}=262$ pm) reacts with the porphyrin to form the homodinuclear mercury(II) porphyrin, $[Hg_2(tpps)(CH_3COO)_2]^{4-}$ ($r_{Hg-N}=222$ pm, $r_{Hg-O}=265$ pm), with a deformed structure, where two mercury(II) bind to two pyrrole nitrogens from upper and lower sides and pyrrole nitrogens are ruffled. The mercury(II) porphyrin was replaced with the distorted octahedral copper(II) acetato complex ($r_{Cu-O}=197$ pm, $r_{Cu-O}=225$ pm) to form the square planar copper(II) porphyrin, $[Cu(tpps)]^{4-}$ ($r_{Cu-N}=200$ pm). The reaction mechanism of the large catalytic effect of mercury(II) on the copper(II) porphyrin formation is discussed from the structure of $Hg_2(tpps)^{2-}$, and the structure of the heterodinuclear intermediate, $[Hg(tpps)Cu]^{2-}$, is proposed.

The rate of metalloporphyrin formation is several orders of magnitude slower than that of open-chain ligands,[1] and the overall mechanism is not simple in some cases.[2,3] However, in the presence of mercury(II), cadmium(II) or lead(II) rapid metallation occurs,[4] and mercury(II) exerts the largest catalytic effect among them.[5] In the metalloporphyrin formation catalyzed by the metal ions, the ionic radius ($r$) of the metal ion acting as catalyst is important. Large metal ions such as $Hg^{2+}$ ($r=114$ pm), $Cd^{2+}$ ($r=95$ pm), and $Pb^{2+}$ ($r=118$ pm) give rise to appreciable catalytic effect, while medium-sized metal ions like $Cu^{2+}$ ($r=73$ pm) and $Zn^{2+}$ ($r=75$ pm) exert hardly the catalytic effect. In the manganese(II) porphyrin formation catalyzed by cadmium(II), cadmium(II) enhances the reaction by a factor of 7900 and a heterodinuclear metalloporphyrin, where cadmium(II) and manganese(II) bind to porphyrin simultaneously, was proposed as an intermediate.[6] The heterodinuclear metalloporphyrin was detected kinetically in the reaction of zinc(II) or copper(II) with homodinuclear mercury(II) porphyrin complex of tetrakis(4-sulfonatophenyl)porphyrin ($H_2tpps^{4-}$).[7] The following biphasic reaction is observed:

$$[Hg_2(tpps)]^{2-} + Cu^{2+} \rightarrow [Hg(tpps)Cu]^{2-} + Hg^{2+} \rightarrow [Cu(tpps)]^{4-} + 2Hg^{2+} \quad (1)$$

The first-step reaction in Eq. 1 completes in a few seconds and it is followed by the second-step reaction with a half-life time of a few minutes.[7]

In order to study structure of chemical species in solution as related to the reaction mechanism, extended X-ray absorption fine structure (EXAFS) measurements have been undertaken for the metal-substitution reaction of mercury(II) porphyrin with copper(II) in an acetate buffer (pH=5.8). Mercury(II) cannot incorporate well into the porphyrin core, and just sits on the porphyrin plane. In addition, mercury(II) is so large that distortion of the porphyrin core is expected.[8] X-Ray analyses of the solid complexes of lead(II) and cadmium(II) porphyrins have shown that lead(II) and cadmium(II) are displaced above from the plane of the porphyrin, 117 pm and 65 pm, respectively.[9,10] The formation of homodinuclear mercury(II) porphyrin has been demonstrated from an $^1H$ NMR study in solution[11] and an X-ray analysis of *N*-substituted porphyrin in solid.[12] In the present study, we will characterize the structure of the reactants ($[Hg_2(tpps)]^{2-}$ and $Cu^{2+}$) and the products ($[Cu(tpps)]^{4-}$ and $Hg^{2+}$) of Eq. 1 in solution, and discuss the catalytic effect of the large metal ions on the metalloporphyrin formation from the structure of the mercury(II)–porphyrin complex with proposing a structure of the heterodinuclear metalloporphyrin as an intermediate.

## Experimental

**Sample Solution.** All chemicals used were of analytical reagent grade and $H_6tpps$ was used without further purification.

Nine test solutions A to I were prepared for EXAFS measurements as given in Table 1. All solutions contained 0.5 mol dm$^{-3}$ $CH_3COONa$ and 0.2 mol dm$^{-3}$ $CH_3COOH$ except for solutions G, H, and I. Solution A is an aqueous mercury(II) acetate solution. Two sample solutions B and C, in which the homodinuclear mercury(II) porphyrin complex is present as the main species, were prepared by dissolving $Hg(CH_3COO)_2$ and $H_2tpps^{4-}$ in water at different molar ratios ($C_{tpps}/C_{Hg}$). These solutions are the reactants for the metal-substitution reaction with copper(II) (solution D). Solutions E and F were prepared by addition of copper(II) acetate to mercury(II) porphyrin solutions. The solution E and F correspond to the metal-substitution reaction of the mercury(II) porphyrin with copper(II), and they contain the reaction products of the mercury(II) acetato and

Table 1. The Composition ($mol\,dm^{-3}$) of Sample Solutions[a)]

| Solution | $Hg(CH_3COO)_2$ | $Cu(CH_3COO)_2$ | $tpps^{6-}$ |
|---|---|---|---|
| A | 0.20 | — | — |
| B | 0.20 | — | 0.10 |
| C | 0.20 | — | 0.20 |
| D | — | 0.10 | — |
| E[b)] | 0.20 | 0.10 | 0.10 |
| F[b)] | 0.20 | 0.20 | 0.20 |
| G[c)] | — | 0.10 | 0.10 |
| H[d)] | 0.20 | — | — |
| I[c)] | — | 0.10 | — |

a) All solutions contained 0.5 $mol\,dm^{-3}$ $CH_3COONa$ and 0.2 $mol\,dm^{-3}$ $CH_3COOH$ except for solutions G, H, and I. b) Copper(II) acetate was added to a mercury(II)–porphyrin solution. c) Copper(II) nitrate was used. d) Mercury(II) nitrate was used.

copper(II) porphyrin complexes. Solution G is an aqueous solution of copper(II) porphyrin, which was prepared by mixing copper(II) nitrate and porphyrin in water and by heating. Solutions H and I are aqueous mercury(II) nitrate and copper(II) nitrate solutions, respectively, and they were used as the structure standard for the Hg–O and Cu–O atom pairs involving the $[Hg(H_2O)_6]^{2+}$ and $[Cu(H_2O)_6]^{2+}$ ions of the known structure.[13—15)]

**EXAFS Measurements.** EXAFS spectra were measured around the Hg $L_{III}$ or Cu K edge in transmission mode using the BL10B station at the Photon Factory of the National Laboratory for High Energy Physics.[16)] A broad band synchrotron radiation was monochromatized by an Si(311) channel-cut crystal. Sample solutions were held in a 3 or 5 mm thick Teflon cell with polyethylene windows and the cell was placed between the first and the second ionization chambers. The apparent absorbance $\mu x$ is obtained as $\ln(I_0/I)$, where $I$ and $I_0$ are X-ray intensities with and without a sample, respectively. Intensities $I_0$ and $I$ were simultaneously measured by the first and the second ionization chambers, respectively. The first ionization chamber was filled with $N_2$ and $N_2(85\%)+Ar(15\%)$ gas in the Cu K- and Hg $L_{III}$-edges, respectively, and the second one with $N_2(75\%)+Ar(25\%)$ and Ar gas in the corresponding edges.

Details of the data reduction of raw EXAFS spectra have been described previously.[17,18)] The threshold energy $E_0$ was selected as the position of the half height of the edge jump in each sample. A curve fitting procedure in the $k$ space for the refinements of structure parameters was applied to the Fourier filtered $k^3\cdot\chi(k)_{obsd}$ values to minimize $\Sigma k^6(\chi(k)_{obsd}-\chi(k)_{calcd})^2$. The model function $\chi(k)_{calcd}$ was obtained according to the single-electron and single-scattering theory.[19—22)] The values of the backscattering amplitude $f(\pi,k)$ were quoted from the literature.[23)] The total scattering phase shift $\alpha(k)$ was approximated by the function $a_0+a_1k+a_2k^2+a_3/k^3$,[24)] where the coefficients $a_0$, $a_1$, $a_2$, and $a_3$ were evaluated by fitting the function to the theoretical phase shift values.[23)] The $E_0$ value is usually treated as a parameter and was evaluated from structure standard for the Cu K-edge spectra. For the Hg $L_{III}$-edge spectra, however, the bond length between mercury(II) ion and ligand atom in the standard sample examined in the present study was hardly reproducible by the refinement of the $E_0$ value, and thus the $a_0$ and $a_1$ values were refined instead of the usual $E_0$ optimization. In the fitting procedures these parameters as well as the $\lambda$ (the mean free path of a photoelectron) value were determined from the standard sample of the known structure and then they were kept constant in the course of the structural analysis of unknown samples, while the interatomic distance $r$, the Debye–Waller factor $\sigma$, and the number of scatters $n$ were optimized as variables.

## Results

Figures 1 and 2 depict the Hg $L_{III}$-edge EXAFS spectra in the form of $k^3\cdot\chi(k)$ of sample solutions and their Fourier transforms (uncorrected for the phase shift), respectively. The first intense peaks observed in the $|F(r)|$ curves in Fig. 2 are due to the Hg–O and/or Hg–N bonds in the first coordination sphere of the mercury(II) ion. The peak position for solutions A, B, C, E, and F shifts to significantly short $r$ as compared with solution H containing the octahedrally hydrated $[Hg(H_2O)_6]^{2+}$ ion.[13)] Hence, the mercury(II) ions in solutions A, B, C, E, and F have a smaller coordination number than six because the ionic radii of metal ions are generally smaller under an environment with a smaller coordination number.[25)] Also, the peak height of solutions B and C, which contained the homodinuclear mercury(II) porphyrin complex as the predominant species regardless of the $C_{tpps}/C_{Hg}$ ratios,[8)] is smaller than that of solutions A, E, and F, in which some species of mercury(II)

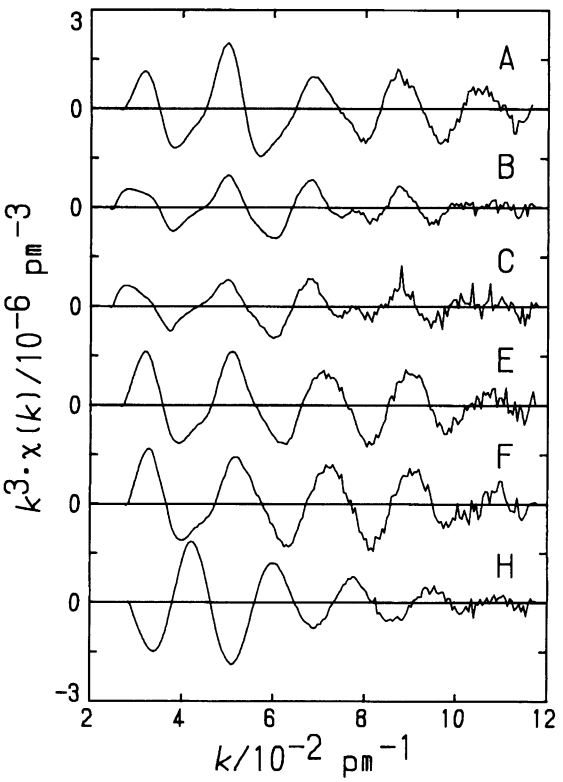


Fig. 1. The extracted Hg $L_{III}$-edge EXAFS spectra in the form of $k^3\cdot\chi(k)$ for sample solutions.

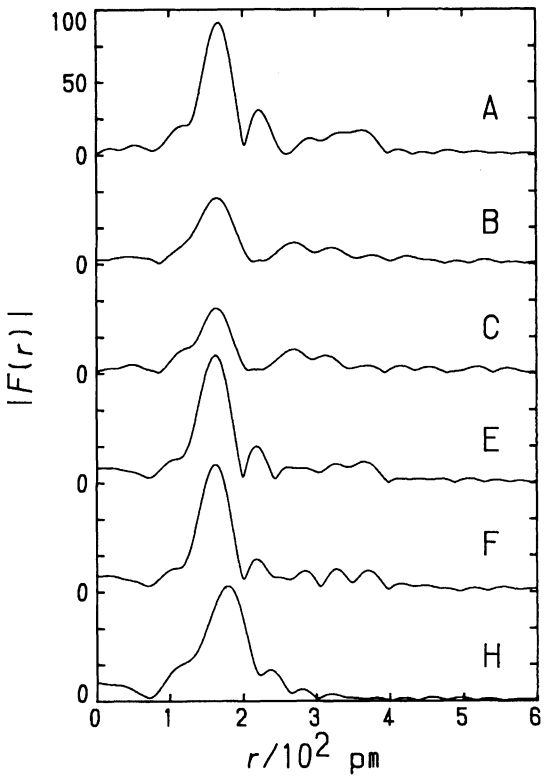


Fig. 2. The radial structure functions $|F(r)|$ of the $k^3 \cdot \chi(k)$ curves shown in Fig. 1, where the phase shift is not corrected.

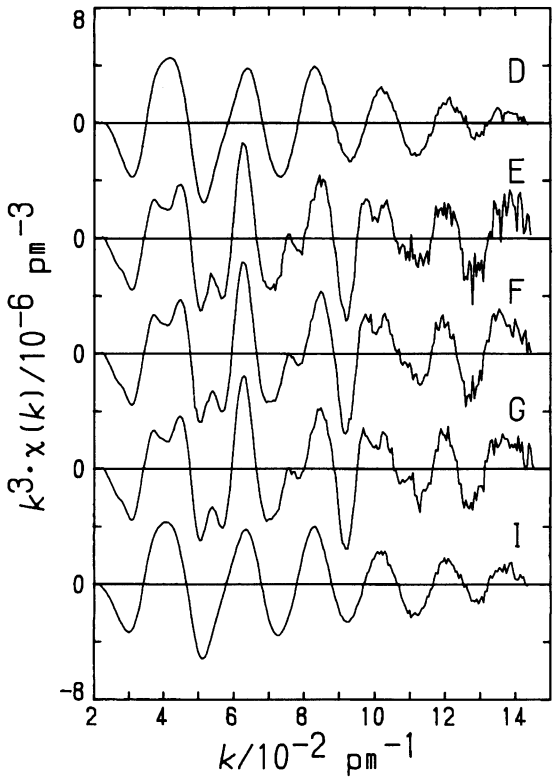


Fig. 3. The extracted Cu K-edge EXAFS spectra in the form of $k^3 \cdot \chi(k)$ for sample solutions.

acetato complexes are present.[26] Thus, the coordination number of mercury(II) within the mercury(II) porphyrin complex is smaller than that within the mercury(II) acetato complexes.

Figures 3 and 4 depict the Cu K-edge EXAFS spectra of sample solutions and their Fourier transforms, respectively. The first peaks in the $|F(r)|$ curves in Fig. 4 are due to the Cu–O and/or Cu–N bonds in the first coordination sphere of the copper(II) ion. The electronic spectrum of the copper(II) acetate solution (solution D) exhibits an absorption maximum at 745 nm ($\varepsilon$=38 mol$^{-1}$ dm$^3$ cm$^{-1}$, while the copper(II) nitrate solution (solution I) at 810 nm ($\varepsilon$=12 mol$^{-1}$ dm$^3$ cm$^{-1}$), in which the $[Cu(H_2O)_6]^{2+}$ ion is present. Thus, the copper(II) ions in solution D formed some copper(II) acetato complexes. Since the shapes of first peak in the $|F(r)|$ curves are virtually the same for solutions D and I (see Fig. 4), the copper(II) acetato complexes in solution D have an axially elongated octahedral structure similar to the $[Cu(H_2O)_6]^{2+}$ ion.[14,15] The $|F(r)|$ curves of solutions E, F, and G are very similar to each other over the wide range of $r$ as seen in Fig. 4. The copper(II) porphyrin complex formed in solutions E and F after the metal-substitution has the same structure as that of an aqueous solution of the copper(II) porphyrin complex (solution G).

The structure parameters of complexes in the first coordination sphere were finally determined by a curve fit in the $k$ space. The Fourier filtering was performed over the $r$ range to include the main peak in the $|F(r)|$ curve for each sample. A least-squares calculation was then applied to the filtered $k^3 \cdot \chi(k)$ values over the range $5.0 < k/10^{-2}$ pm$^{-1} < 11.0$ for the Hg $L_{III}$-edge spectra and $5.0 < k/10^{-2}$ pm$^{-1} < 13.5$ for the Cu K-edge spectra. The phase function and the $\lambda$ value for Hg–O and Cu–O atom pairs were evaluate from solutions H and I containing the $[Hg(H_2O)_6]^{2+}$ and $[Cu(H_2O)_6]^{2+}$ ions, respectively, of the known structure.[13—15] The bond length, the Debye–Waller factor, and the coordination number of the complexes were then refined as independent variables by adopting the $\lambda$ value and the phase function evaluated above. The results are summarized in Tables 2 and 3, and the solid curves in Figs. 5 and 6 calculated by using the parameter values well reproduced the experimental points.

## Discussion

**Structure of Mercury(II) Complexes.** The mercury(II) ions in solution A exist as a mixture of some species of mercury(II) acetato complexes.[26] The $k^3 \cdot \chi(k)$ values of solution A were well reproduced considering two kinds of the Hg–O bonds, i.e., Hg–O ($CH_3COO^-$) and Hg–O ($H_2O$). The bond having a shorter length must be ascribed to the Hg–O ($CH_3COO^-$) one since the mercury(II)–anion interaction is stronger than the mercury(II)–water one. The Hg–O ($CH_3COO^-$) bond length of 219 pm is much shorter and the Hg–O ($H_2O$)

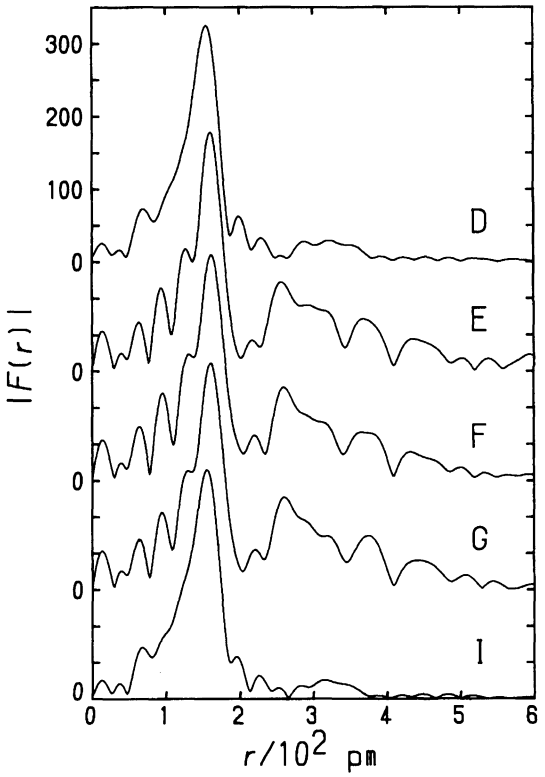


Fig. 4. The radial structure functions $|F(r)|$ of the $k^3 \cdot \chi(k)$ curves shown in Fig. 3, where the phase shift is not corrected.

Table 2. Results of the Least-Squares Refinements for Structure Parameters of the Mercury(II) Complexes[a)]

| Solution | Interaction | $r$/pm | $\sigma$/pm | $n$ |
|---|---|---|---|---|
| A | Hg–O | 219(1) | 7.0(3) | 2.4(1) |
| | Hg–O | 262(2) | 12(2) | 1.7(5) |
| B | Hg–N | 222(1) | 8.6(1) | 2.0(2) |
| | Hg–O | 265(2) | 10(3) | 0.7(4) |
| C | Hg–N | 223(1) | 8.9(5) | 2.2(3) |
| | Hg–O | 260(3) | 11(3) | 0.7(5) |
| E | Hg–O | 214(1) | 7.6(3) | 2.4(2) |
| | Hg–O | 254(2) | 9(1) | 1.3(3) |
| F | Hg–O | 213(3) | 7.7(4) | 2.3(2) |
| | Hg–O | 252(2) | 8(1) | 1.5(3) |
| H | Hg–O | 241[b)] | 11.4(1) | 6[b)] |

a) The values in parentheses represent standard deviation. b) The values were kept constant during the calculations.

one of 262 pm is much longer than that (241 pm) of the $[Hg(H_2O)_6]^{2+}$ ion.[13)] The number of the Hg–O ($CH_3COO^-$) bond is 2.4 as shown in Table 2. The fractional number is interpreted in terms of the presence of comparable amounts of the diacetatomercury(II) and triacetatomercurate(II) complexes. Also, the sum of acetate and water molecules bound to mercury(II) is nearly four and thus the structure of the di- and triacetato complexes is four-coordinate tetrahedral.

The number of the Hg–N and Hg–O bonds converged

Table 3. Results of Least-Squares Refinements for Structure Parameters of Copper(II) Complexes[a)]

| Solution | Interaction | $r$/pm | $\sigma$/pm | $n$ |
|---|---|---|---|---|
| D | Cu–O | 197(1) | 7.4(1) | 4.4(1) |
| | Cu–O | 225(1) | 10.1(5) | 2.1(2) |
| E | Cu–N | 200(1) | 5.2(1) | 3.6(1) |
| F | Cu–N | 200(1) | 4.9(1) | 3.5(1) |
| G | Cu–N | 200(1) | 4.8(1) | 3.5(1) |
| I | Cu–O | 197(1) | 6.8(1) | 4[b)] |
| | Cu–O | 224(1) | 10.9(1) | 2[b)] |

a) The values in parentheses represent standard deviation. b) The values were kept constant during the calculations.

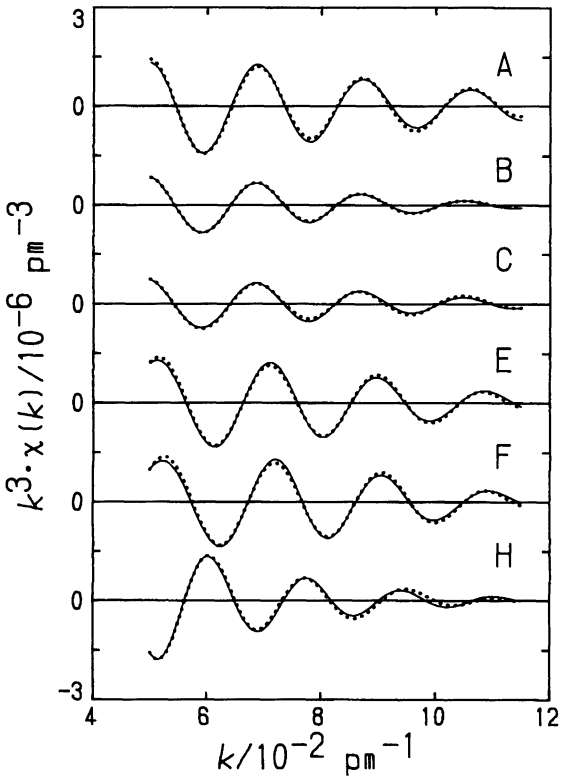


Fig. 5. The Fourier filtered $k^3 \cdot \chi(k)$ curves of the main peak shown in Fig. 2. The observed and calculated values are shown by dots and solid lines, respectively.

to almost two and one, respectively, for both solutions B and C containing the homodinuclear mercury(II) porphyrin complex (see Table 2.) The Hg–O bond is attributable to the Hg–O ($CH_3COO^-$) one rather than Hg–O ($H_20$). Each mercury(II) ion within the complex is coordinated with two nitrogen atoms and an acetate ion. The three-coordinate structure around the mercury(II) ion is thus suggested for the homodinuclear mercury(II) porphyrin complex on the basis of the total number of the Hg–N and Hg–O bonds. The Hg–N and Hg–O bond lengths are 223(2) and 263(6) pm, respectively. In a solution of mercury(II) nitrate and porphyrin, the mercury(II) ion is coordinated with two nitrogen atoms and 2—3 water molecules and the Hg–

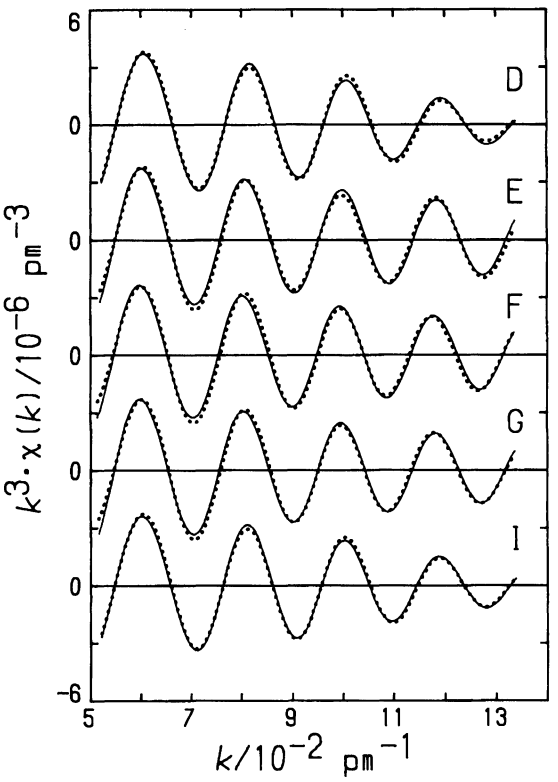


Fig. 6. The Fourier filtered $k^3 \cdot \chi(k)$ curves of the main peak shown in Fig. 4. The observed and calculated values are shown by dots and solid lines, respectively.

N and Hg–O ($H_2O$) bond lengths are 215 and 255 pm, respectively.[8] The Hg–N bond length is elongated and thus the bond is weakened by the binding of an acetate ion, but the Hg–O bond length in $[Hg_2(tpps)(CH_3COO)_2]^{4-}$ becomes longer by a little due, probably, to a steric hindrance between the methyl group of acetate and the phenyl proton of the porphyrin.

The mercury(II) ions after mixing of the mercury(II)–porphyrin complex with the copper(II) ion (solutions E and F) give rise to the mercury(II) acetato complexes as well as the copper(II) porphyrin complex. The length, the Debye–Waller factor, and the number of the Hg–O bonds are quite similar for solutions E and F as expected (Table 2). Based on the sum of the number of the Hg–O ($CH_3COO^-$) and Hg–O ($H_2O$) bonds, the mercury(II) acetato complexes in solutions E and F have a four-coordinate tetrahedral structure as well as in solution A. However, the Hg–O bond lengths of the mercury(II) acetato complexes in solutions E and F are different from those of solution A. The Hg–O ($CH_3COO^-$) bond length is shortened and the Hg–O ($H_2O$) one is elongated in solutions E and F compared with solution A. The total concentration of acetate ions in solutions E and F was larger than that in solution A (see Table 1). Thus, the different result of solutions E and F from that of solution A may be caused by the different acetate concentration, i.e., the concentration of the di- or triacetato complex of mercury(II) in solutions E and F increased compared with that in solution A.

**Structure of Copper(II) Complexes.** According to the electronics spectra described in the previous section, the copper(II) ions in solutions D exist as a mixture of some species of copper(II) acetato complexes. Also, these copper(II) acetato complexes exhibit a distorted octahedral structure like the $[Cu(H_2O)_6]^{2+}$ ion. The distorted octahedral structure of the copper(II) acetato complexes is also supported by the fact that the number of the equatorial and axial Cu–O bonds of the copper(II) acetato complexes in solution D are almost four and two, respectively, as shown in Table 3. The equatorial and axial Cu–O bond lengths in the copper(II) acetato complexes are 197(1) and 225(1) pm, respectively, and are the same as those in the $[Cu(H_2O)_6]^{2+}$ ion.

The EXAFS spectrum of an aqueous solution of copper(II) porphyrin (solution G) was well explained by an introduction of one kind of Cu–N interaction and a further introduction of the Cu–O interaction did not cause any improvement in the curve fit, i.e., no evidence for the coordination of water molecules to the copper(II) ion was found. The number of the Cu–N bond converged to almost four and the copper(II) ion is coordinated with four nitrogen atoms of porphyrin in an aqueous solution. The structure of the copper(II) porphyrin complex is thus four-coordinate square planar and the Cu–N bond length is 200(1) pm. The four-coordinate square planar structure has been revealed for the copper(II) tetrapropylporphyrin complex in crystal and the Cu–N bond length is 200 pm,[27] which is the same as that in aqueous solution. The structure parameters of the copper(II) porphyrin complex formed after the metal-substitution (solutions E and F) is quite similar to each other. Thus, the same discussion for solution G can be applied to solutions E and F. The copper(II) porphyrin complex of the reaction product has a four-coordinate square planar structure.

**Metal-Substitution Reaction.** The structure of copper(II) porphyrin is hardly affected by the metal-substitution reaction, because of the rigid and stable structure of the cooper(II) porphyrin. However, the bond lengths of the mercury(II) porphyrin and mercury(II) acetato complexes depended on the composition of solution or coordinated atom. The possible structural change during the reaction of $[Hg_2(ttps)]^{2-}$ with $Cu^{2+}$ is postulated as in Scheme 1. The tetrahedral mercury(II) acetato complex reacts with $H_2ttps^{4-}$ to form the homodinuclear mercury(II) porphyrin complex with the deformed structure, where two mercury(II) bind to two pyrrole nitrogens from upper and lower sides and one acetate anion coordinates to each mercury(II). The pyrrole rings are twisted alternatively up and down like "saddle" porphyrin skeleton,[28] and deviated 30° from the mean porphyrin plane, The nonbonded Hg···Hg distance is estimated to be 310 pm

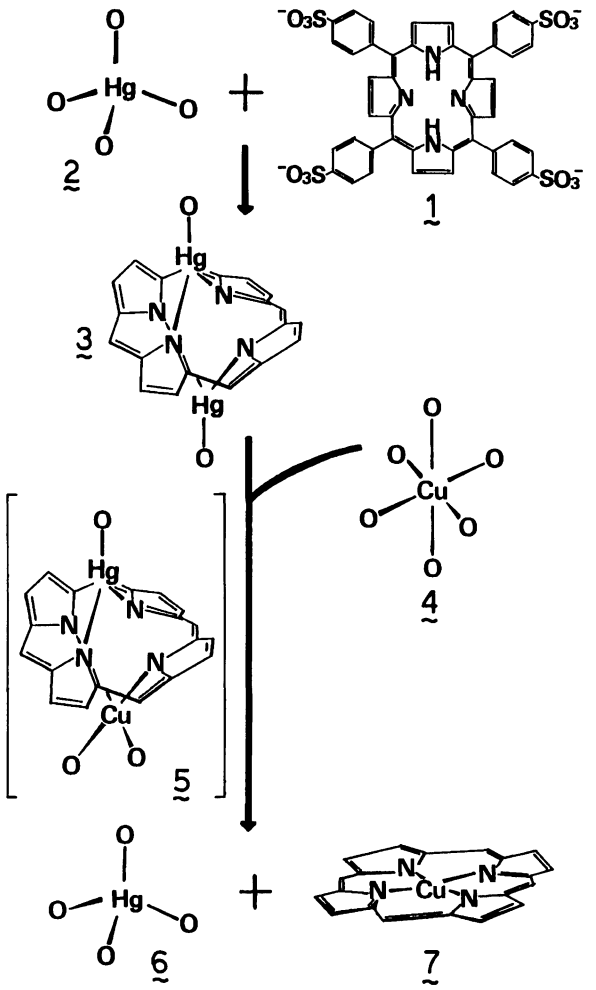

Scheme 1. Reaction scheme of the metal-substitution reaction of $Hg_2(tpps)^{2-}$ with copper(II) in an acetate buffer. 1, free base porphyrin; 2, mercury(II) acetato complex; 3, homodinuclear mercury(II) porphyrin; 4, copper(II) acetato complex; 5, heterodinuclear intermediate; 6, mercury(II) acetato complex; 7, copper(II) porphyrin.

by taking into account of nonplanarity of the pyrrole rings. The mercury(II) porphyrin is easily replaced by the copper(II) acetato complex having a distorted octahedral structure and forms the copper(II) porphyrin through the heterodinuclear intermediate.

For divalent transition metal ions, the rate constant for metalloporphyrin formation is about $10^3$ times less reactive than *N*-methylated porphyrin which is further $10^3$ times less reactive than 1,10-phenanthlorine.[4] The extremely slow rate of the metalloporphyrin formation is due to the rigidity of porphyrins. Since cyclic ligands like porphyrin are not flexible, porphyrin ring should be distorted to accept the incoming metal ion at the pyrrole nitrogen atom. An X-ray analyses of *N*-substituted porphyrin complex indicates that the *N*-substituted pyrrole ring is deviated by about 40° from the average porphyrin plane.[29] The present EXAFS study also suggests the pronounced distortion in the mercury(II)–porphyrin complex, $[Hg_2(ttps)]^{2-}$: the pyrrole ring is canted by about 30° from the average porphyrin plane. Thus the lone-pair electrons on pyrrole nitrogen in the deformed structure are available to incoming metal ion to form the heterodinuclear intermediate. The structures of the heterodinuclear metalloporphyrin intermediate have not been known, but we have elucidated the formation of the heterodinuclear metalloporphyrin complex as an intermediate, where mercury(II) and copper(II) or zinc(II) bind to a porphyrin simultaneously, from the the kinetic analysis and a rapid-scan spectrophotometry of the biphasic kinetic-run for the reaction of $[Hg_2(tpps)]^{2-}$ with $Cu^{2+}$ or $Zn^{2+}$.[7] Similar intermediate has also been suggested by Robinson and Hambright.[30] Very recently, Ohtaki, et al. have directly detected, by using a stopped flow EXAFS, the structure of the heterodinuclear metalloporphyrin as an intermediate.[31] Mercury(II) binds to only two pyrrole nitrogen atoms, leaving other pyrroles free to copper(II) as in the structure of the homodinuclear mercury(II) porphyrin complex, $[Hg_2(ttps)]^{2-}$. The structure of $[Hg_2(ttps)]^{2-}$ is deformed and one mercury(II) ion is continually being released and reformed. Copper(II) ion could attack the 1:1 mercury(II)–porphyrin complex from the opposite side to mercury(II) and forms the heterodinuclear metalloporphyrin complex as an intermediate. We have repeatedly reported that large metal ions like $Hg^{2+}$, $Cd^{2+}$ and $Pb^{2+}$ enhance the formation of metalloporphyrin and mercury(II) exerts the largest catalytic effect on the metalloporphyrin formation.[4—6] The present study indicates that the binding of mercury(II) to porphyrin deforms porphyrin ring and that the deformation may make it easy to accept the incoming metal ion resulting in the formation of the heterodinuclear metalloporphyrin as an intermediate. This is the reason why large metal ions accelerate the metalloporphyrin formation rate.

EXAFS measurements have been performed under the approval of the Photon Factory Program Advisory Committee (Proposal No. 90-159). The present study was partly supported by Grant-in-Aid for Scientific Research on Priority Area No. 04215218 from the Ministry of Education, Science and Culture.

## References

1) D. W. Margerum and G. R. Caylley, "Coordination Chemistry," ed by A. E. Martell, American Chemical Society, Washington, DC (1978), pp. 1—194.

2) D. K. Lavallee, *Coord. Chem. Rev.*, **61**, 55 (1985).

3) D. K. Lavallee, *Comments Inorg. Chem.*, **5**, 155 (1986).

4) M. Tabata and M. Tanaka, *Trends Anal. Chem.*, **10**, 128 (1991).

5) M. Tabata and M. Tanaka, *Inorg. Chim. Acta Lett.*, **1980**, X71.

6) M. Tabata and M. Tanaka, *J. Chem. Soc., Dalton*

*Trans.*, **1983**, 1955.
7) M. Tabata and W. Miyata, *Chem. Lett.*, **1991**, 785.
8) M. Tabata and K. Ozutsumi, *Bull. Chem. Soc. Jpn.*, **65**, 1438 (1992).
9) K. M. Barkigia, J. Fajer, A. D. Adler, and G. J. B. Williams, *Inorg. Chem.*, **19**, 2057 (1980).
10) P. F. Rodesiler, E. A. H. Griffith, N. G. Charles, and E. L. Amma, *Inorg. Chem.*, **24**, 4595 (1985).
11) M. F. Hudson and K. M. Smith, *J. Chem. Soc., Chem. Commun.*, **1973**, 515.
12) H. J. Callot, B. Cherrier, and R. J. Weiss, *J. Am. Chem. Soc.*, **101**, 7729 (1979).
13) G. Johansson, *Acta Chem. Scand.*, **25**, 2787 (1971).
14) H. Ohtaki, T. Yamaguchi, and M Maeda, *Bull. Chem. Soc. Jpn.*, **49**, 701 (1976).
15) M. Nomura and T. Yamaguchi, *J. Phys. Chem.*, **92**, 6157 (1988).
16) M. Nomura, "KEK Report 85- 7," National Laboratory for High Energy Physics, Tsukuba (1985).
17) K. Ozutsumi and T. Kawashima, *Inorg. Chim. Acta*, **180**, 231 (1991).
18) K. Ozutsumi, Y. Miyata, and T. Kawashima, *J. Inorg. Biochem.*, **44**, 97 (1991).
19) D. E. Sayers, E. A. Stern, and F. W. Lytle, *Phys. Rev. Lett.*, **27**, 1204 (1971).
20) E. A. Stern, *Phys. Rev. B*, **10**, 3027 (1974).
21) E. A. Stern, D. E. Sayers, and F. W. Lytle, *Phys. Rev. B*, **11**, 4836 (1975).
22) B. Lengelar and P. Eisenberger, *Phys. Rev. B*, **21**, 4507 (1980).
23) B. -K. Teo and P. A. Lee, *J. Am. Chem. Soc.*, **101**, 2815 (1979).
24) P. A. Lee, B. -K. Teo, and A. L. Simons, *J. Am. Chem. Soc.*, **99**, 3856 (1977).
25) R. D. Shannon, *Acta Crystallogr., Sect. A*, **32**, 751 (1976).
26) A. E. Martell and R. M. Smith, "Critical Stability Constants," Plenum Press, New York (1977), Vol. 3.
27) I. Moustakali and A. Tulinsky, *J. Am. Chem. Soc.*, **95**, 6811 (1973).
28) K. M. Barkigia, M. D. Berber, J. Fajer, C. J. Medforth, M. W. Renner, and K. M. Smith, *J. Am. Chem. Soc.*, **112**, 8851 (1990).
29) D. K. Lavellee, "The Chemistry and Biochemistry of *N*-Substituted Porphyrins," VCH Publishers, New York (1987).
30) L. R. Robinson and P. Hambright, *Inorg. Chem.*, **31**, 652 (1992).
31) H. Ohtaki, Y. Inada, S. Funahashi, M. Tabata, K. Ozutsumi, and K. Nakajima, *J. Chem. Soc., Chem. Commun.*, in press.